

How to write a good research paper

Bill Freeman

MIT CSAIL

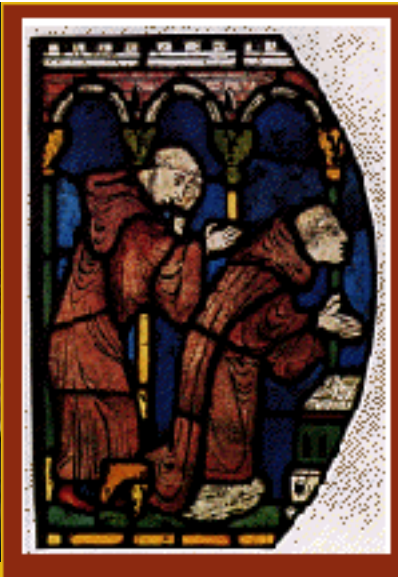
Nov. 29, 2018

A paper's impact on your career



Our image of the research community

- Scholars, plenty of time on their hands, pouring over your manuscript.



The reality:
more like a large, crowded marketplace



<http://ducksflytogether.wordpress.com/2008/08/02/looking-back-khan-el-khalili/>

Ted Adelson on how to write a good paper

- (1) Start by stating which problem you are addressing, keeping the audience in mind. They must care about it, which means that sometimes you must tell them why they should care about the problem.
- (2) Then state briefly what the other solutions are to the problem, and why they aren't satisfactory. If they were satisfactory, you wouldn't need to do the work.
- (3) Then explain your own solution, compare it with other solutions, and say why it's better.
- (4) At the end, talk about related work where similar techniques and experiments have been used, but applied to a different problem.

Since I developed this formula, it seems that all the papers I've written have been accepted. (told informally, in conversation, 1990).

Example paper organization: removing camera shake from a single photograph

1 Introduction

2 Related work

3 Image model

4 Algorithm

Estimating the blur kernel

Multi-scale approach

User supervision

Image reconstruction

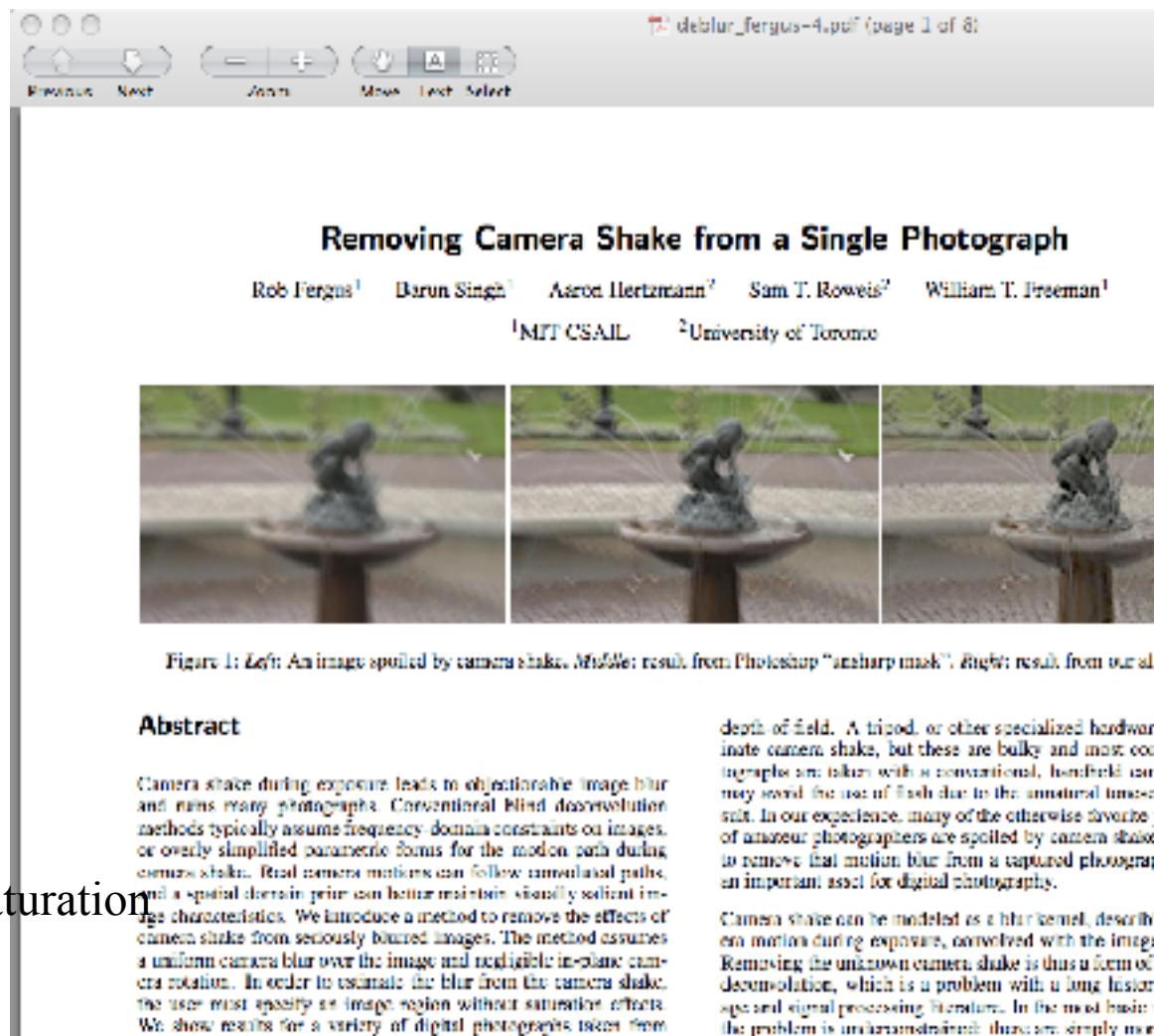
5 Experiments

Small blurs

Large blurs

Images with significant saturation

6 Discussion



The image shows a PDF viewer window with the title page of a paper. The title is "Removing Camera Shake from a Single Photograph". The authors listed are Rob Fergus¹, Barun Singh¹, Azrael Hertzmann², Sam T. Roweis², and William T. Freeman¹. The affiliations are ¹MIT CSAIL and ²University of Toronto. Below the title and authors, there are three side-by-side images of a fountain. The left image is blurry, the middle image is the result of Photoshop's "unsharp mask", and the right image is the result of the proposed method, which is sharper than the Photoshop result. Below the images is the abstract, which discusses the problem of camera shake during exposure and the proposed method for removing it. The abstract mentions that conventional methods typically assume frequency-domain constraints on images, or overly simplified parametric forms for the motion path during camera shake. It also mentions that real camera motions can follow unanticipated paths, and a spatial domain prior can better maintain visually salient image characteristics. The proposed method introduces a method to remove the effects of camera shake from seriously blurred images. The method assumes a uniform camera blur over the image and negligible in-plane camera rotation. In order to estimate the blur from the camera shake, the user must specify an image region without saturation effects. The paper shows results for a variety of digital photographs taken from

depth of field. A tripod, or other specialized hardware, can avoid the use of flash due to the unnatural timescale. In our experience, many of the otherwise favorite of amateur photographers are spoiled by camera shake to remove that motion blur from a captured photograph, an important asset for digital photography.

Camera shake can be modeled as a blur kernel, describing motion during exposure, convolved with the image. Removing the unknown camera shake is thus a form of deconvolution, which is a problem with a long history and signal processing literature. In the most basic, the problem is unconstrained; thus, one simply uses

Removing Camera Shake from a Single Photograph

Witajczyk¹ Janszky¹ Amini-Harandi² Sarti ¹ Weiss² Williams¹

¹MIT CSAIL ²University of Toronto



FIGURE 1. LEFT: ORIGINAL IMAGE BY CHRIS STRAL. MIDDLE: RESULTING SHARPENED ORIGINAL IMAGE. RIGHT: RESULTING DEBLURRED

Abstract

Camera shake during exposure leads to objectionable image blur and ruins many photographs. Conventional blind deconvolution methods typically assume frequency-domain constraints on images or overly simplified parametric forms for the motion path during camera motion. Real camera motions can follow complex paths and a camera cannot prior to better maintain visually pleasing image characteristics. We introduce a method to remove the effects of camera shake from not only blurred images. The method assumes constant camera blur over the image and integrates exposures over motion. In order to estimate the blur from the camera shake the user must specify an image region without occlusion effects. We show results for a variety of digital photographs taken from personal stills collections.

CC Categories: 1.4.3 [Image Processing and Computer Vision] E.5.5 [Image Processing and Computer Vision] I.2.10 [Artificial Intelligence]: Learning

Keywords: camera shake, blind image deconvolution, variational learning, motion image statistics

1 Introduction

Camera shake, in which an unstably mounted camera blurs photographs, is a chronic problem for photographers. The experience of consumer digital photography has made camera shake very prominent, particularly with the popularity of small, high-resolution cameras whose light weight can make them difficult to hold as heavily used. Many photographs capture important moments that cannot be repeated under controlled conditions or repeated with different camera settings. If camera shake occurs in the image for any reason, then the moment is “lost”.

Shake can be mitigated by using longer exposures, but this can lead to other problems such as sensor noise or a smaller time frame

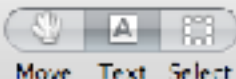
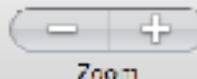
depth-of-field. A tripod or other specialized hardware can eliminate camera shake, but these are bulky and most consumer photographs are taken with a conventional, handheld camera. Users may need the use of hardware to the greatest extent possible for visual image acquisition, many of the other well-known alternatives of consumer photographers are caused by camera shake. A method to remove that motion blur from a captured photograph would be an important asset for digital photography.

Camera shake can be modeled as a blur kernel, derived by the camera motion during exposure, convolved with the image intensities. Removing the unknown camera shake is thus a form of blind image deconvolution, which is a problem with a long history in the image and signal processing literature. In the most basic formulation, the problem is unconstrained: there are simply more unknowns (the original image and the blur kernel) than measurements (the observed image). Hence, all practical solutions must make strong prior assumptions about the blur kernel, about the image to be recovered, or both. Traditional signal processing formulations of the problem usually make only very general assumptions in the form of frequency-domain power laws, or modeling spatio-temporal blur as either smooth or with corner sharp. Furthermore, algorithms involving linear priors restricted to the Fourier domain can not properly represent spatial-domain structures such as edges.

This paper introduces a new technique for removing the effects of unknown camera shake from an image. This process results from another measurement over motion blur. First, we compute motion statistics in several image statistics, which shows that photographs of natural scenes typically obey very specific distributions of image gradients. Second, we build on work by Sapiro and MacKinnon [2006], adopting a Bayesian approach that uses an explicit uncertainty in the unknowns, allowing us to find the blur kernel implied by a distribution of possible images. From this kernel, the image is then reconstructed using a standard Richardson-Lucy method, although we believe there is room for substantial improvement in this reconstruction phase.

We assume that all image blur is descriptive (meaning convolution, i.e., there is no significant parallel, any image-plane motion of the camera is small, and no part of the scene is moving relative to any another during the exposure). Our approach currently requires a small amount of runtime.

Our reconstruction is capable of being, particularly when the



these two approaches are valid; however, they may be acceptable to researchers in some cases, and a practitioner might choose one or the other. In contrast, the original images are typically available, beyond reaching up — in fact our method may help “rescue” data that would have otherwise been completely lost.

2 Related Work

The task of deblurring images is nontrivial, especially if the blur is not known. In this problem, it will be “blind”. For a survey on the literature in this area, see [Kundur and Srinivasan 1998], including some comprehensive methods, especially those that use the fast Fourier transform (FFT) as well as a Gaussian low-frequency “mask” component. However, as discussed by our examples, the blur kernel induced during camera shake is not a simple blur, and also contains very sharp edges. Similar non-stationary assumptions are typically made for the input image, e.g., applying a quadratic regularization. Such assumptions are proven high frequency (such as edges) from appearing in the reconstruction. Cases et al. [2002] assume a sparse low distribution on the image magnitude power spectrum as a simple form of natural image statistics for the joint image-to-image analysis. Some notable extensions to this problem include [2003, Hough and Lee 2003] (assume power laws with variable exponents) for the case when the complete blur kernel is not known.

Convolution methods have been developed for astronomical images [Osh 1998, Xie and Jan 1997, Thompson et al. 1994, Zelnick 1995], which have statistical quite different from the natural scenes we address in this paper. Performing blind deconvolution in this domain is usually straightforward, as the blurry image is an isolated star against an irrelevant background.

Another approach is to assume that there are multiple images available of the same scene [Bridier et al. 1996, Bar, Aho, and Szeliski 1997]. Hardware approaches include optically induced blurs [Camerlino, 1995], specially designed CMOS sensors [Liu and Qian 2001], and hybrid imaging systems [Bridier et al. and Fienberg 1997]. Since we would like to extend to work with existing cameras and imaging and to work for as many situations as possible, we do not investigate any such advanced techniques available.

Some work is concerned about how to solve the problem of over-sampled images given as a variety of applications, including focusing [Koh and Lee 2006], super-resolution [Tippin et al. 2004, Murray and Weiss 2005], video motion [Kanehisa et al. 2004, Flanagan 2002, Linschinske, Levin et al. 2003], and scattering reduction [Liu and Weiss 2004]. Indeed, these authors effectively “see-blind”, in that the image formation process (e.g., the size variation, over-sampling) is assumed to be known or recoverable. While and Mackay [2000] perform blind deconvolution on the raw images with a prior on the ideal intensities. Some of us shows an initial attempt of professional application. We apply a similar “non-blind” scheme for natural images using image gradients in place of intensities, and adapted the algorithm to achieve results for probability images and statistical data.

3 Image model

Our algorithm takes as input a blurred image B , which is assumed to have been generated by convolution of a blur kernel K with a latent image L , as follows:

$$B = K * L + N \quad (1)$$

where $*$ denotes image convolution (with appropriate boundary conditions), and N denotes sensor noise at each pixel. We assume that the pixel values of the image are linearly related to

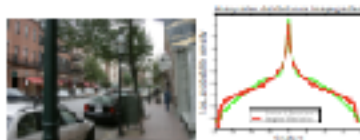


Figure 2: Left: A natural scene image. Right: The magnitude of gradient magnitudes with the scene, as shown in red. The y-axis has a logarithmic scale, it shows the heavy tails of the distribution. The nature of Gaussian approximation used in our estimation is clear in green.

the sensor hardware. The latent image L represents the image we would have captured if the camera had captured perfectly, and our goal is to recover L from B without specific knowledge of K .

In order to estimate the latent image from such blurred images, mean, it is essential to make some form of which images are a priori more likely. Fortunately, recent research in natural image statistics have shown that, although images of real-world scenes vary greatly in their observed color distributions, they obey canonical distributions in their gradients [Pitlo, 1994]: the distribution of gradients has most of its mass at small values but over the slightly more probability to large values than a Gaussian distribution. This corresponds to the literature that images of an object large sections of random elements in pixel intensity gradient locations, by over-sampled large elements in color or colorless boundaries. For example, Figure 2 shows a natural image and a histogram of its gradient magnitudes. The distribution shows that the magnitudes primary consist of very gradients, but a few pixels have very large magnitudes. Recent image processing methods based on heavy-tailed distributions (i.e., non-Gaussian models) in image denoising [Forn and Black 2005, Srinivasan 2005] and in representation [Tippin et al. 2004] in recent methods based on Gaussian prior distributions (including natural image statistics) produce much smoother images.

We represent the distribution over gradient magnitudes with a zero-mean mixture-of-Gaussians model, as illustrated in Figure 2. This representation was chosen because of our previous prior experience with the empirical distribution, while allowing a standard optimization problem for our algorithm.

4 Algorithm

There are two main steps in our approach. First, the blur kernel is estimated from the input image. The estimation process is performed via a non-iterative method in order to avoid local minima. SECOND, USING THE ESTIMATED KERNEL, WE APPLY A STANDARD CONVOLUTIONAL algorithm to estimate the latent (unknown) image.

The new approach has inputs to the algorithm: the blurred image B , a rectangular patch within the blurred image, an upper bound on the size of the blur kernel (in pixels), and an initial guess on the estimation of the blur kernel (boundary values). Details of how we modify these assumptions are given in Section 4.1.2.

Additionally, we require input image B to have been converted to a linear color space before processing. In our experiments, we applied inverse gamma correction¹ with $\gamma = 2.2$. In order to estimate the gradient of the kernel, we compute all the color channels of the original image, which for each specified patch to produce a projected blurred patch P .

¹Real value = 2000 inverse value^{1.7}

4.1 Estimating the blur kernel

Given the grayscale blurred image P , we estimate K and the latent patch image L_0 by finding the values with highest probability, as guided by a prior on the statistics of L . Since these statistics are shared by the image gradient rather than the intensity, we reformulate the optimization in the gradient domain, using ∇L_0 and ∇P for the gradients of L_0 and P . Because convolution is a linear operation, the patch gradient ∇P should be equal to the convolution of the latent gradient with the kernel: $\nabla P = \nabla L_0 * K$, and since we assume that this kernel function with constant σ^2

As discussed in the previous section, the prior $p(\nabla L_0)$ on the latent image gradients is a mixture of C zero-mean Gaussians (with means μ_i and widths λ_i for $i = 1, \dots, C$ elements). We use a mixture prior $q(K)$ for the kernel that encourages area values in the central region of values to be positive. Specifically, the prior on central values is a mixture of C independent distributions with mean factors λ_i and weights α_i for $i = 1, \dots, C$ elements:

Given the blurred image gradient ∇P , we use variational Bayesian distributions over the unknowns with fixed μ_i :

$$p(K, \nabla L_0 | \nabla P) \propto p(\nabla P | K, \nabla L_0) p(\nabla L_0) q(K) \quad (2)$$

$$= \prod_{i=1}^C \mathcal{N}(\nabla L_0 | \mu_i, \lambda_i \nabla \nabla L_0) \prod_{i=1}^C \mathcal{N}(K | \lambda_i) \quad (3)$$

$$\prod_{i=1}^C \mathcal{N}(\nabla L_0 | \mu_i, \lambda_i \nabla \nabla L_0) \prod_{i=1}^C \mathcal{N}(K | \lambda_i)$$

where λ_i denotes each image patch and λ_i denotes each blur kernel element. A real kernel K does not have separate real and imaginary components. For simplicity, we assume that the gradients in ∇P are independent of each other, so we treat the elements in ∇L_0 and K .

A straightforward approach to maximization is to solve for the maximum a-posterior (MAP) solution, which finds the kernel K and latent image gradient ∇L_0 that maximize $p(K, \nabla L_0 | \nabla P)$. We avoid this for a variety of reasons: our search space is too large to attempt to fit the data while also minimizing small gradients. We would like to incorporate gradient priors (as found by the image prior above) into optimization in the MAP objective function, to minimize local gradients over large areas, whereas we expect natural images to have some large gradients. Consequently the algorithm would solve some image, since virtually all the gradients are zero. If we reduce the noise variance (thus increasing the weights in the data fitting terms) then the algorithm yields a delta function for K , which usually has an absurdly large λ_i within an arbitrary region. Additionally, we find the MAP objective function to be very susceptible to poor local minima.

Instead, our approach is to approximate the full posterior distribution $p(K, \nabla L_0 | \nabla P)$ and then sample the kernel K with maximum marginal probability. This method selects a kernel that is most likely with respect to the distribution of possible latent images, thus avoiding the overfitting that can occur when selecting a single “best” estimate of the image.

IN ORDER TO DESIGN THE APPROXIMATION EFFICIENTLY, WE ADAPT A VARIATIONAL Bayesian approach [Jordan et al. 1999] which computes a distribution $q(K, \nabla L_0)$ that approximates the posterior $p(K, \nabla L_0 | \nabla P)$. In particular, we approximate based on Minka and MacKay’s algorithm [Minka and MacKay 2001] for rapid convergence of variational approximations (based on $q(K, \nabla L_0) = q(K)q(\nabla L_0)$). For the blur image gradients, this approximation is a Gaussian family, while for the noise variance (the kernel elements), it is a mixture of Gaussians. The distributions for each blur kernel and the latent elements are represented by their mean and variance, which is an array.

Following Minka and MacKay [2001], we also need the covariance matrix σ^2 of an unknown (using the variational process, this means the one from taking the variational). This allows the entire variance to vary during estimation; the one being constant is loose only in the process, however, tighter or better, low noise variance is more likely. We place a prior on σ^2 in the form of a uniform distribution on the inverse variance, using hyper-parameters α, β : $p(\sigma^2) \propto \beta^\alpha (\alpha/\sigma^2)^{-\alpha} \exp(-\beta/\sigma^2)$. The variational covariance of σ^2 is also a Gaussian distribution.

The variational algorithm minimizes a cost function representing the unknowns. In approximating the likelihood and the true posterior, measured as $\mathcal{KL}(q(K, \nabla L_0, \sigma^2) || p(K, \nabla L_0 | \nabla P))$. The independence assumption in the variational posterior allows the cost function to be defined:

$$\mathcal{KL}(q(K, \nabla L_0, \sigma^2) || p(K, \nabla L_0 | \nabla P)) \propto \sum_{i=1}^C \left[\frac{\alpha_i}{\lambda_i} \log \frac{\alpha_i}{\lambda_i} + \frac{\beta}{\lambda_i} \log \frac{\beta}{\lambda_i} \right] + \sum_{i=1}^C \left[\frac{\alpha_i}{\lambda_i} \log \frac{\alpha_i}{\lambda_i} + \frac{\beta}{\lambda_i} \log \frac{\beta}{\lambda_i} \right] \quad (4)$$

where $\lambda_i \propto \sigma^2$ denotes the covariance with respect to σ^2 . The kernel K is dependent on σ^2 is omitted from the expression.

The cost function is then minimized as follows. The means of the distribution K and ∇L_0 are set to the initial values of K and ∇L_0 and the variance of the distributions are high, including the lack of coupling in the initial estimate. The parameters of the distributions are then updated iteratively by coordinate descent, as outlined by alternating one over the other while increasing the cost function. Updates are performed by computing closed-form optimal posterior estimates, and performing line search in the direction of these optimal values (see Appendix A for details). The updates are repeated until the change in \mathcal{KL} becomes negligible. The final set of marginal distributions $\mathcal{KL}(K, \nabla L_0 | \nabla P)$ is then used to find the best value for K . Our implementation adapts the source code provided online by Minka and MacKay [2006].

In our formulation outlined above, we have approximated the probability of observed pixels in the image, as well as our linearly related values, our model. Since dealing with non-negativity is essential, we prefer to simply mask our estimated regions of the image during the inference procedure, so that we do not cause of them.

For the variational framework, $\mathcal{L} = \mathcal{KL}(q(K, \nabla L_0, \sigma^2) || p(K, \nabla L_0 | \nabla P))$, the parameters at the place on the blur image gradients λ_i, μ_i were estimated first, a single latent image, lower λ_i values, using EM. Since the image statistics vary across scale, each scale had its own set of prior parameters. The prior was used for the approximation. The parameters for the mean in the blur kernel elements were estimated from a small set of low-resolution images inferred from our images.

4.1.1 Multi-scale approach

The algorithm described in the previous section is subject to local minima, particularly for large blur kernels. Hence, we perform optimization by varying image resolutions in a coarse to fine manner. At the coarsest level, K is a 3×3 kernel. To ensure a coarse start to the algorithm, we usually specify the initial 3×3 blur kernel to use of some simple patterns (see Section 4.1.2). The initial estimate for the latent patch image is also provided by sampling the latent scene, while holding K fixed.

We first work back up to a small resolution (the inference at each level, the averaged values of K and ∇L_0 being upsampled from an initialization) for inference at the next scale up. At the final scale, the inference converges to the full resolution kernel K .

²For example, $\sigma^2 = \frac{1}{\lambda_i} \log \frac{\alpha_i}{\lambda_i} + \frac{\beta}{\lambda_i} \log \frac{\beta}{\lambda_i} + \frac{\alpha_i}{\lambda_i} - \beta$.

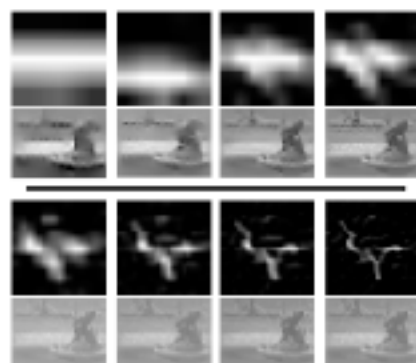


Figure 3: The multi-scale inference scheme operating on the fountain image in Figure 1. Top & Left rows: The estimated blur kernel at each scale level. 2nd & 3rd rows: Estimated image patch at each scale. The intensity image was reconstructed from the gradient used in the inference using Poisson image reconstruction. The Poisson reconstructions are shown for reference only; the final reconstruction is found using the Richardson-Lucy algorithm with the final estimated blur kernel.

4.1.2 User supervision

Although it would seem more natural to run the multi-scale inference scheme using the full gradient image ∇I , in practice we found the algorithm performed better if a smaller patch, rich in edge structure, was manually selected. The manual selection allows the user to avoid large areas of saturation or uniformity, which can be disruptive or uninformative to the algorithm. Examples of user-selected patches are shown in Section 5. Additionally, the algorithm runs much faster on a small patch dataset of entire images.

An additional parameter is that of the maximum size of the blur kernel. The size of the blur encountered in images varies widely, from a few pixels up to hundreds. Small blurs are used to resolve if the algorithm is initialized with a very large kernel. Conversely, large blurs will be corrected if too small a kernel is used. Hence, an operation under all conditions, the approximate size of the kernel is a required input from the user. By examining any blur artifact in the image, the size of the kernel is easily deduced.

Finally, we also require the user to select between one of two initial estimates of the blur kernel: a horizontal line or a vertical line. Although the algorithm can often be initialized in either state and still produce the correct, high resolution kernel, this ensures the algorithm starts searching in the correct direction. The appropriate initialization is easily determined by looking at any blur kernel artifact in the image.

4.2 Image Reconstruction

The multi-scale inference procedure outputs an estimate of the blur kernel \mathbf{K} , marginalized over all possible image reconstructions. To recover the defocused image given this estimate of the kernel, we experimented with a variety of non-blind deconvolution methods, including those of Gerchik [1992], Nedunuri [2006] and van Cittert [Zarevitz 1996]. While many of these methods perform well in

synthetic test examples, our real images exhibit a range of non-linearities not present in synthetic ones, such as non-Gaussian noise, saturated pixels, residual non-linearities in cross-scale and estimation errors in the kernel. Disappointingly, when run on our images, most methods produced unacceptable levels of artifacts.

We also used our variational inference scheme on the gradient of the whole image ∇I , while holding \mathbf{K} fixed. The intensity image was then formed via Poisson image reconstruction [Wells 2001]. Aside from being slow, the inability to model the non-linearities mentioned above resulted in reconstructions no better than other approaches.

As \mathbf{I} typically is large, speed sensitive to non-single method structure. Consequently, we reconstructed the latent color image \mathbf{L} with the Richardson-Lucy (RL) algorithm [Richardson 1972; Lucy 1974]. While the RL performed comparably to the other methods evaluated, it has the advantage of taking only a few minutes, even on large images (other more complex methods, took hours or days). RL is a non-blind deconvolution algorithm that iteratively maximizes the likelihood function of a Poisson statistics image noise model. One benefit of this over more direct methods is that it gives only non-negative output values. We use Matlab's implementation of the algorithm to estimate \mathbf{L} , given \mathbf{K} , treating each color channel independently. We used 10 RL iterations, although for large blur kernels, more may be needed. Before running RL, we clamp \mathbf{K} by applying edge-aware denoising, based on our maximum-likelihood value within the kernel which sets all elements below a certain value to zero, so reducing the overall noise. The output of RL, whether gamma-corrected using $\gamma = 2.2$ and its intensity histogram matched to that of \mathbf{I} (using Matlab's `histeq` function), resulting in \mathbf{L} . See pseudo-code in Appendix A for details.

5 Experiments

We performed an experiment to check that blurry images are mainly due to camera translation as opposed to other motions, such as in-plane rotation. To this end, we asked 4 people to photograph a whiteboard³ which had small black dots placed in each corner while using a shutter speed of 1 second. Figure 4 shows dots extracted from a random sampling of images taken by different people. The dots in each corner reveal the blur kernel lead to that portion of the image. The blur patterns are very similar, showing that our assumption of quickly invariant blur with little in-plane rotation is valid.

We apply our algorithm to a number of real images with varying degrees of blur and saturation. All the photos were from personal photo collections, with no exception of the amateur and cafe images which were taken with high-end DSLR using long exposures ($> 1/2$ seconds). For each we show the blurry image, followed by the output of our algorithm along with the estimated kernel.

The running time of our algorithm is dependent on the size of the patch selected by the user. With the minimum practical size of 128×128 it currently takes 30 minutes in our Matlab implementation. For a patch of N pixels, the runtime is $O(N \log N)$ owing to our use of FFT's to perform the convolution operations. Hence larger patches will still run in a reasonable time. Compiled and optimized versions of our algorithm could be expected to run considerably faster.

Small blur. Figures 4 and 6 show run on images degraded by small blurs that are significantly sharper by our algorithm. The

³Camera-to-whiteboard distance was 50 cm. Lens focal length was 50mm mounted on a 0.6 ISLR lens.

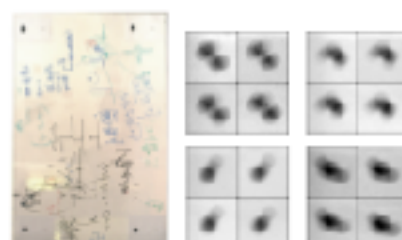


Figure 5: Left: The whiteboard test scene with dots in each corner. Right: Kernels from the corners of images taken by different people. Within each image, the dot trajectories are very similar, suggesting the image blur is well modeled as a quickly invariant translation.

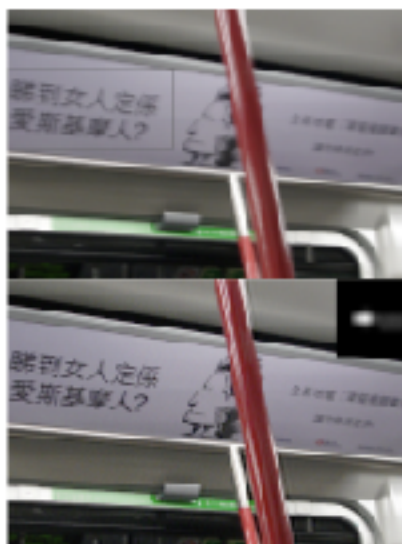


Figure 6: Top: A scene with a small blur. The patch selected by the user is indicated by the gray rectangle. Bottom: Output of our algorithm and the inferred blur kernel. Note the crop text.

gray rectangles show the patch used to infer the blur kernel, chosen to have many in-focus pixels but few saturated pixels. The inferred kernels are shown in the corner of the deburred images.

Large blurs. Unlike existing blind deconvolution methods our algorithm can handle large, complex blurs. Figures 7 and 8 show our algorithm successfully inferring large blur kernels. Figure 7 shows an image with a complex in-focus blur. 30 pixels in size shown in Figure 10) being defocused.

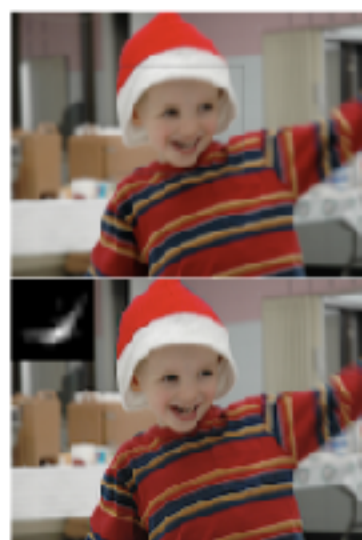


Figure 7: Top: A scene with complex motions. While the camera is small, the child is both translating and, in the time, rotating. Bottom: Output of our algorithm. The white rectangle shows the area around the blur kernel estimated by our algorithm.

As demonstrated in Figure 8, the true blur kernel is uncovered in the image by the trajectory of a pointlight source formed by the blur. This gives us an opportunity to compare our blur kernel with the true one. Figure 10 shows image structures, along with the inferred kernels, from the five images.

We also compared our algorithm against existing blind deconvolution algorithms, running Matlab's described blind restoration procedure, implementations of the methods of Briggs and [1986] and Irwin [1997]. Based on the iterative Richardson-Lucy scheme, these methods also estimate the blur kernel, along with the image, holding the blur invariant and updating the image versus. The results of this algorithm, applied to the fountain scenes are shown in Figures 11 and are more comparable to other algorithms, shown in Figures 1 and 12.

Images with significant saturation. Figures 12 and 13 show large areas where the true intensities are not observed to the dynamic range limitations of the camera. The user patch used for kernel analysis must avoid the large saturated areas. While the deburred image does have some still saturated regions, the unsaturated regions can still be extracted.

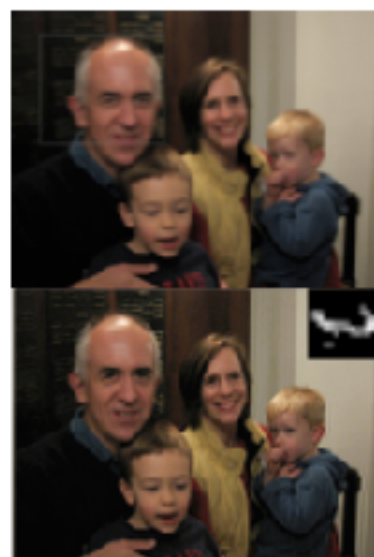
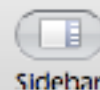
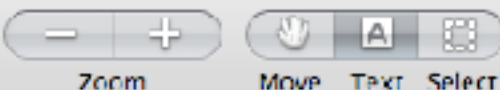


Figure 7: Top: A scene with a large blur. Bottom: Output of our algorithm. See Figure 1 for a close-up view.

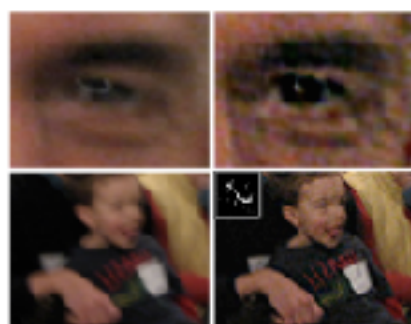


Figure 8: Top row: Closeup of the man's eye in Figure 7. The original image (on the left) shows a speedlight artifact caused by the camera motion. In the deblurred image (on right), the speedlight is condensed to a point. The color noise artifacts due to low light exposure can be removed by median filtering the chrominance channels. Bottom row: Closeup of child from another image of the family (4 frames from Figure 7). In the deblurred image, the text on his jersey is now legible.



Figure 9: Top: A blurry photograph of three children. Bottom: Output of our algorithm. The fine detail of the wallpaper is now visible.

6 Discussion

We have introduced a method for removing camera shake effects from photographs. This problem appears highly understudied at first. However, we have shown that by applying natural image priors and advanced statistical techniques, plausible results can nonetheless be obtained. Such an approach may prove useful in other computational photography problems.

Most of our effort has focused on kernel estimation, and, visually, the kernels we estimate seem to match the image camera motion. The results of our method often consist of artifacts; most prominently, ringing artifacts occur near saturated regions and regions of significant object motion. We suspect that these artifacts can be blamed primarily on the non-blind deconvolution step. We believe that there is significant room for improvement by applying modern statistical methods to the non-blind deconvolution problem.

There are a number of common photographic effects that we do not explicitly model, including saturation, object motion, and compression artifacts. Incorporating these issues into our model should improve robustness. Currently we assume images do have a linear threshold, once the gamma correction has been removed. However, cameras typically have a slight sigmoidal shape to their tone response curve, so to improve their dynamic range. Ideally, this non-linearity would be removed, perhaps by estimating it during inference, or by measuring the curve from a series of bracketed

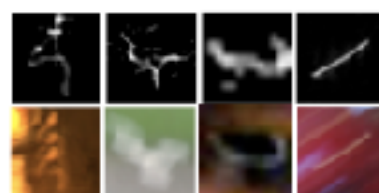


Figure 10: Top row: Inferred blur kernels from four different images (the cat, fountain and family scenes plus another image not shown). Bottom row: Images extracted from these scenes while the true kernel has been revealed. In the cat image, low light gives a dual image of the kernel. In the fountain scene, a white square is transformed by the blur kernel. The final two images have speedlights transformed by the camera motion, revealing the true kernel.



Figure 11: Baseline experiments, using Matlab's blind deconvolution algorithm (`deconvblind`) on the fountain image (top) and cat image (bottom). The algorithm was initialized with a Gaussian blur kernel, similar in size to the true artifacts.

resources. Additionally, our method could be extended to make use of more advanced natural image statistics, such as correlations between color channels, or the fact that camera motion traces a continuous path (and thus arbitrary kernels are not possible). There is also some room to improve the noise model in the algorithm; our current approach is based on Gaussian noise in image gradients, which is not a very good model for image sensor noise.

Although our method requires some manual intervention, we believe these steps could be minimized by employing more exhaustive search procedures, or heuristics to guess the relevant parameters.



Figure 12: Top: A normal scene with significant saturation. The long thin region caused by the sun has been cut out or 'restored' output of our algorithm. Note the double exposure type blur kernel.

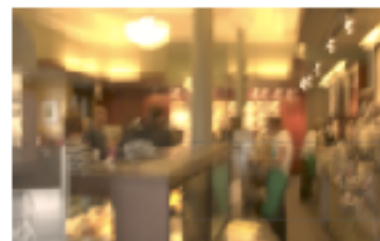


Figure 13: Top: A blurred scene with heavy saturation, taken with a 1 second exposure. Bottom: Output of our algorithm.

Acknowledgements

We are indebted to Antonio Tormba, Don Casas and Fredo Durand for their insights and suggestions. We are most grateful to James McMahon and David McKay, for making their code available online. We would like to thank the following people for supplying us with blurred images for the paper: Chris Kwan, Reinhard Klein, Michael Laswicki, Pietro Pezzoni and Elizabeth Van Ruitenberk. Funding for the project was provided by NSERC, NFA NSERC 1562 GS 0064 and the Shell Group.

References

Arce, G., and Penedorero, A. 2004. Bayesian video denoising using loopy image priors. In *Conf. on Computer Vision and Pattern Recognition*, 407-411.

BALOGH, D., BAYLIS, A., AND DORRINGTON, A. 1995. Motion-Peeking and Super-Resolution from an Image Sequence. In *ICCV* (2), 473-483.

BIDAKOVA, S., AND TURK, D. R. 2004. Motion-Blurred Motion Delineation. *CVPR*. *Proc. on Conference on Computer Vision and Pattern Recognition*, 20, 4, 699-701.

BRENN, D., AND ANDERSON, M. 1995. Acceleration of Iterative Image Restoration Algorithms. *Applied Optics*, 34, 8, 1750-1773.

CANNON, J., 2006. What happened image denoising? <http://www.cse.cuhk.edu.hk/~jcannon/>.

CHEN, J., ZHANG, N., AND HULLIGY, C. 2002. Noniterative video denoising by use of an structure prior function. *APPLIED OPTICS*, 41, 22, 3960-3964.

FRICK, D. 1994. Noise-free gradient images coding. *Image Computation*, 5, 579-581.

VOLKMAN, D., AND RUIJTER, W. 1992. Consistent smoothing and denoising of distributions. *IEEE Trans. on Pattern Analysis and Machine Intelligence* 14, 3, 371-383.

GILL, E. 1998. Bayesian inference, inference and maximum entropy. In *Maximum Entropy and Bayesian Methods*, 3, Skilling, J., Ed. Kluwer, 39-71.

DEGHAN, A., BLANC-FRANCO, L., AND ZHOU, J. 2002. Estimation of blur and tone parameters in image denoising. In *Proc. of the Conference on Speech and Signal Processing*.

JEON, J. A. 1997. *Development of Incoherent Spectra*. Academic Press.

JORDAN, M., GRAHAMER, Z., JANKOVA, T., AND SAUL, L. 1999. An introduction to variational methods for graphical models. In *Machine Learning*, vol. 17, 103-223.

K. SUDA, R., AND RAJENDRA, D. 1998. Mod frame reconstruction. *IEEE Trans. Pattern Analysis and Machine Intelligence* 20, 3, 349-364.

LING, A., AND WISE, E. 2004. User-Aided Segmentation of Reflections from a Single Image Using a Stochastic Prior. In *CVPR*, vol. 1, 403-410.

LING, A., ZHANG, A., AND WISE, E. 2005. Learning How to Ignore from Global Image Statistics. In *CVPR*, vol. 1, 77.

LI, K., AND CHANG, A. 2001. Simultaneous image denoising and restore the nonlocal self-similarity property. In *Proc. of Conf. on Computer Vision, Pattern Recognition and Applications*, 3, 1161-1164.

LI, Y., J. 2004. Bayesian-based iterative method of image denoising. *Journal of Astronomy*, 30, 746-754.

MARTEL, P., AND MARKESS, D. J. C. 1990. *Iterative Learning for Blind Image Separation and Deconvolution. In Advances in Adaptive Computer Graphics*, M. Grasse, Ed. Springer-Verlag.

MARTEL, P. 2000. This iterative image denoising process. http://www.cse.cuhk.edu.hk/~jcannon/papers/this_iterative_image_denoising.pdf.

MARTEL, P. 2005. *Iterative Learning for Adaptive Computer Graphics*. PhD thesis, University of Waterloo.

NONAKAWA, H., CHEN, R., AND KAWANAMI, H. 2004. Parallel Fourier methods for the blind denoising of 3D-compressed videos. *IEEE Trans. on Signal Processing*, 52, 579-592.

ROTHWATER, P., AND BAYLIS, R. 2004. The nonlocalized image as blur-free class. *Pattern Recognition Letters*, 25, 111-113.

RUJTER, W. 1991. Bayesian-based iterative method of image restoration. *Journal of the Optical Society of America*, 8, 2, 25-28.

RUFF, L., AND ELBAK, H. L. 2003. Fusion of Synthetic Aperture Radar for Learning Image Priors. In *CVPR*, vol. 1, 890-895.

SCHNEIDERLI, E. 2005. Statistical denoising of geographic images. In *Workshop on Image and Video Processing*, A. Rosenfeld, Ed. 4.

LUPSON, M. P., SCHNEIDERLI, E., AND BERMAN, W. L. 2005. Exploiting the sparse structure prior for super-resolution and image denoising. In *ICCV*.

THANUMAYAN, P., MULLA, N., AND BURR, N. 1994. Iterative blur deconvolution method using a priori information. *IEEE Transactions on Image Processing*, 3, 12, 1619-1629.

WELLS, J. 1991. Deriving intrinsic image from image sequences. In *ICCV*, 68-73.

ZHANG, W. 1994. Robust, consistent, and computationally efficient restoration of van Cittert deconvolution optical blurring. *Journal of the Optical Society of America A*, 11, 11, 2106-2113.

Appendix A

Here we give pseudo code for the algorithm Image Denoiser. This code is the reference version. Unfortunately, adapted from Mishin and McKeay (2006, 2008). For brevity, only the key steps are detailed. Methods notation is used. The Matlab functions `imread`, `imwrite`, and `imshow` are used with their standard syntax.

Algorithm 1 Image Denoiser

Require: Blurry image I , blurred sub-window P , maximum blur size q , overall blur direction $\alpha=0$ or $\pi/4$, $\beta=1$ for some parameter for prior on V_L , $\beta_0 = \{1, 0\}$, parameter for prior on K , $\beta_1 = \{0, 1\}$.

Current P is grayscale.

Input parameters P (default $q=12$).

$V_L = P \otimes [1, -1]$. % Compute gradient in x .

$V_T = P \otimes [1, -i]$. % Compute gradient in y .

$V_P = (V_L, V_T)$. % Composite gradient.

$S = [-2 \sin(\alpha) \cos(\beta)]$. % SP of scale, starting with 3×3 kernel.

for $l = 1$ to K do % Loop over scales, starting at coarsest

V_P subimage of $V_P \otimes [1, 0]$. % $K \times K$ subimage problem

\hat{V} from V_P via % Global least-squares problem

$\hat{V} = \{ \hat{V}_x(x), \hat{V}_y(x), \hat{V}_x(y), \hat{V}_y(y) \}$, $\hat{V}_x = (V_L^T)^T$

$\hat{V}_y = \{ \hat{V}_y(x), \hat{V}_y(y) \}$ % Inference on $V_P \otimes [1, 0]$, keeping K^2 local.

do % Loop over subimage from previous scale

$V_L = \text{subimage}(V_L, \hat{V}_x, \hat{V}_y, \text{kernel})$.

$V_T = \text{subimage}(V_T, \hat{V}_x, \hat{V}_y, \text{kernel})$.

$K = \text{subimage}(K, \hat{V}_x, \hat{V}_y, \text{kernel})$.

end do

$\{K, V_L\} = \text{subimage}(V_P, \hat{V}_x, \hat{V}_y, \text{kernel})$. % Also inference

end for

Set elements of K^l that are less than $\text{mean}(K^l) / 2$ to zero. % Thresholding

$B = \text{subimage}(B, K^l)$. % Another adaptive scaling

$L = \text{subimage}(L, B, K^l)$. % Another adaptive scaling

Denoised image I (initially $= I$).

Histogrammed L or K using `histeq`.

Output: L, K^l .

Algorithm 2 Deconvolution (Global Methods: Mishin and McKeay (2006))

Require: Observed blurry gradient V_P , initial non-zero K , initial zero gradient V_L , blurred prior parameters only, blur gradient prior β_0 .

$N = \text{imsize}(V_P)$, $q = N_x$, $\text{kernel} = q \times q$.

V_P is $N_x \times N_y \times N_c$, $N = N_x \times N_y$, $V_{K_0} = I^T$.

V_L is $L \times L \times N_c$, $N = N_x \times N_y$, $V_{L_0} = I^T$.

$I = I^T \otimes 1$. % Set initial non-zero I

$\mu = [I, I^T \otimes [1, 0], [0, 1], [0, 1]]$. % Initial distribution

repeat

$V^l = \text{subimage}(V_P, \beta_0, \beta_1, \beta_2)$. % Get v^l distribution

$Z^l = V^l - \mu$. % Gradient deviation

$C^l = \text{argmin}_C \|Z^l - \mu - C\mu\|$. % One search

% C is computed using Mishin (2006) Eqn. 5.17-5.19

$\mu = \mu + C^l \mu$. % Update distribution

until Convergence: $\|C^l\|_1 < \epsilon \times 10^3$

$K^l = [K, V_L^l] \otimes [1, 0]$. % Max non-zero

Output: K^l and V_L^l .

$v^l = \text{subimage}(V_P, \beta_0, \beta_1, \beta_2)$.

μ Subimage to compute updated gradient

% Distributional gradient prior across components parameters

$\mu_{x_1} = \mu_{x_1} \otimes [1, 0]$, $\mu_{x_2} = \mu_{x_2} \otimes [0, 1]$, $\mu_{y_1} = \mu_{y_1} \otimes [1, 0]$

$\mu_{y_2} = \mu_{y_2} \otimes [0, 1]$, $\mu_{z_1} = \mu_{z_1} \otimes [1, 0]$, $\mu_{z_2} = \mu_{z_2} \otimes [0, 1]$

$\mu_{z_3} = \mu_{z_3} \otimes [1, 0]$, $\mu_{z_4} = \mu_{z_4} \otimes [0, 1]$, $\mu_{z_5} = \mu_{z_5} \otimes [1, 0]$, $\mu_{z_6} = \mu_{z_6} \otimes [0, 1]$

$\mu_{z_7} = \mu_{z_7} \otimes [1, 0]$, $\mu_{z_8} = \mu_{z_8} \otimes [0, 1]$, $\mu_{z_9} = \mu_{z_9} \otimes [1, 0]$, $\mu_{z_{10}} = \mu_{z_{10}} \otimes [0, 1]$

$\mu = [I^T \otimes 1; Z^l; (V_P - K) \otimes [1, 0]; (V_P - I) \otimes [0, 1]]$. % μ for $v^l = \mu^T$

% Update parameters of v^l

Global analysis function `argmin` [Mishin 2006] page 10, Eqs. A.8 and A.9

$\hat{V}_x(x) = \hat{V}_x(x)$, $\hat{V}_y(y) = \hat{V}_y(y)$, $\hat{V}_x(y) = \hat{V}_x(y)$. % Update parameters of V_L , V_T

$\hat{V}_y(x) = \hat{V}_y(x)$. % Update parameters of V_P

$\mu^l = [I, I^T \otimes [1, 0], [0, 1], [0, 1]]$. % Global gradient

Return: v^l .

The introduction

1 Introduction

2 Related work

3 --Main idea--

4 Algorithm

- Estimating the blur kernel

 - Multi-scale approach

 - User supervision

- Image reconstruction

5 Experiments

- Small blurs

- Large blurs

- Images with significant saturation

6 Discussion

Jim Kajiya: write a dynamite introduction

You must make your paper easy to read. You've got to make it easy for anyone to tell what your paper is about, what problem it solves, why the problem is interesting, what is really new in your paper (and what isn't), why it's so neat. And you must do it up front. In other words, you must write a dynamite introduction.

Underutilized technique: explain the main idea with a simple, toy example.

1 Introduction

2 Related work

3 Main idea

4 Algorithm

Estimating the blur kernel

Multi-scale approach

User supervision

Image reconstruction

5 Experiments

Small blurs

Large blurs

Images with significant saturation

6 Discussion

← Often useful here.

Show simple toy examples to let people get the main idea

From
“Shiftable
multiscale
transforms”

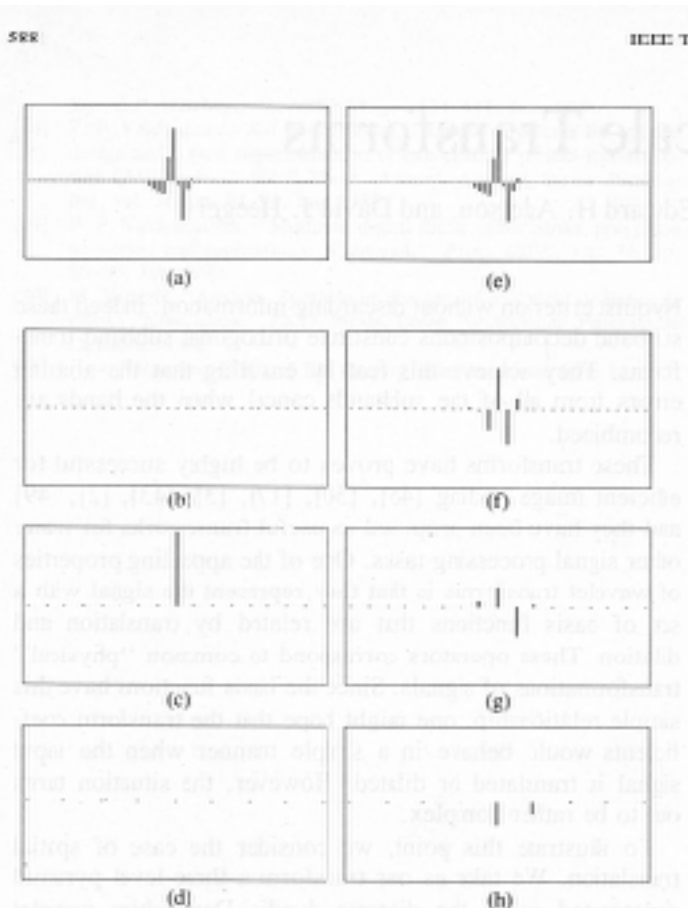


Fig. 1. Effect of translation on the wavelet representation of a signal. (a) Input signal, which is equal to one of the wavelet basis functions. (b)-(d) Decomposition of the signal into three wavelet subbands. Plotted are the coefficients of each subband. Dots correspond to zero-value coefficients. (e) Same input signal, translated one sample to the right. (f)-(h) Decomposition of the shifted signal into three wavelet subbands. Note the drastic change in the coefficients of the transform, both within and between subbands.

Steerable filters simple example

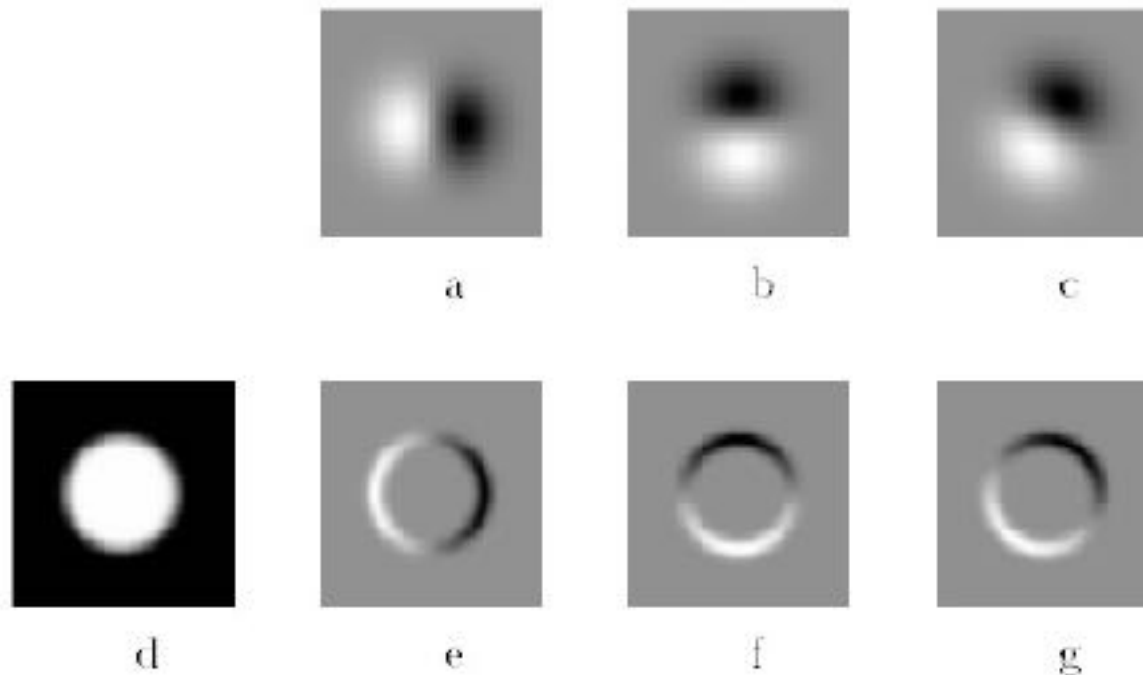


Fig. 1. Example of steerable filters: (a) $G_1^{0^\circ}$ first derivative with respect to x (horizontal) of a Gaussian; (b) $G_1^{90^\circ}$, which is $G_1^{0^\circ}$, rotated by 90° . From a linear combination of these two filters, one can create G_1^θ , which is an arbitrary rotation of the first derivative of a Gaussian; (c) $G_1^{60^\circ}$, formed by $\frac{1}{2}G_1^{0^\circ} + \frac{\sqrt{3}}{2}G_1^{90^\circ}$. The same linear combinations used to synthesize G_1^θ from the basis filters will also synthesize the response of an image to G_1^θ from the responses of the image to the basis filters; (d) image of circular disk; (e) $G_1^{0^\circ}$ (at a smaller scale than pictured above) convolved with the disk (d); (f) $G_1^{90^\circ}$ convolved with (d); (g) $G_1^{60^\circ}$ convolved with (d), obtained from $\frac{1}{2}$ (image (c)) + $\frac{\sqrt{3}}{2}$ (image (f)).

Experimental results are critical now at CVPR

1 Introduction

2 Related work

3 Image model

4 Algorithm

Estimating the blur kernel

Multi-scale approach

User supervision

Image reconstruction

5 Experiments

Small blurs

Large blurs

Images with significant saturation

6 Discussion

Gone are the days of, “We think this is a great idea and we expect it will be very useful in computer vision. See how it works on this meaningless, contrived problem?”

Experimental results from Fergus et al paper



Figure 10: *Top row*: Inferred blur kernels from four real images (the cafe, fountain and family scenes plus another image not shown). *Bottom row*: Patches extracted from these scenes where the true kernel has been revealed. In the cafe image, two lights give a dual image of the kernel. In the fountain scene, a white square is transformed by the blur kernel. The final two images have specularities transformed by the camera motion, revealing the true kernel.

Experimental results from a later deblurring paper

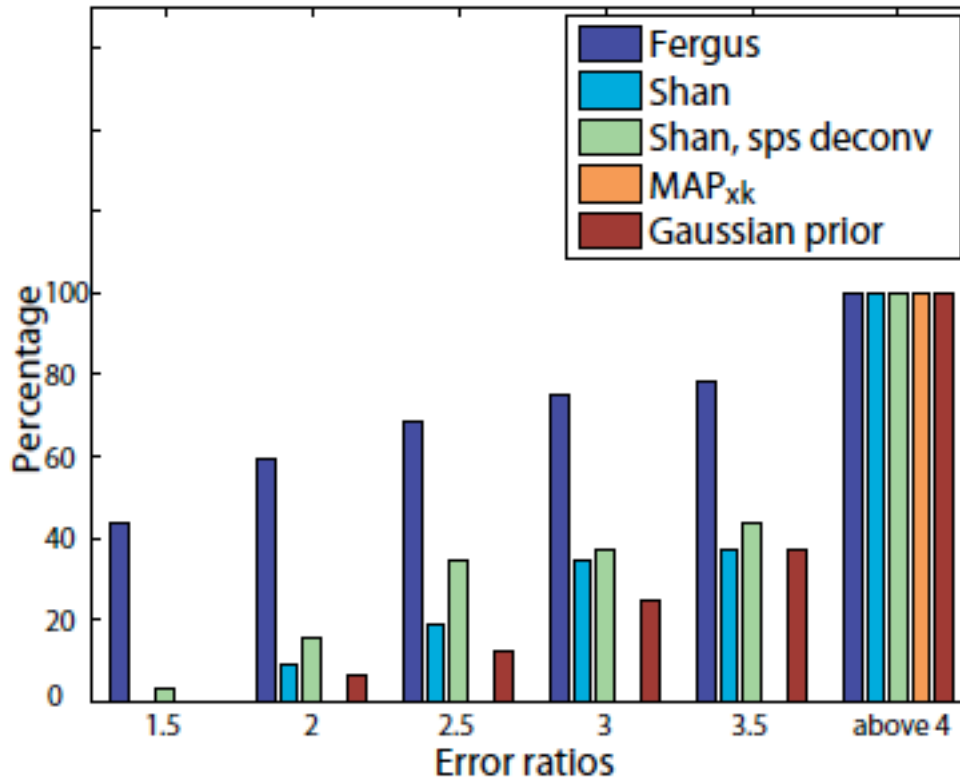


Figure 9. Evaluation results: Cumulative histogram of the deconvolution error ratio across test examples.

How to end a paper

1 Introduction

2 Related work

3 Image model

4 Algorithm

Estimating the blur kernel

Multi-scale approach

User supervision

Image reconstruction

5 Experiments

Small blurs

Large blurs

Images with significant saturation

6 Discussion

Conclusions, or what this opens up, or how this can change how we approach computer vision problems.

How not to end a paper

1 Introduction

2 Related work

3 Image model

4 Algorithm

Estimating the blur kernel

Multi-scale approach

User supervision

Image reconstruction

5 Experiments

Small blurs

Large blurs

Images with saturation

6 Discussion

Future work?

I can't stand "future work" sections.
It's hard to think of a weaker way
to end a paper.

"Here's a list all the ideas we wanted to do but
couldn't get to work in time for the conference
submission deadline. We didn't do any of the
following things: (1)..."

(You get no "partial credit" from reviewers and readers
for neat things you wanted to do, but didn't.)

"Here's a list of good ideas that you should now go
and do before we get a chance."

Better to end with a conclusion or a summary, or you can
say in general terms where the work may lead.

General writing tips

Knuth: keep the reader upper-most in your mind.

12. Motivate the reader for what follows. In the example of §2, Lemma 1 is motivated by the fact that its converse is true. Definition 1 is motivated only by decree; this is somewhat riskier.

Perhaps the most important principle of good writing is to keep the reader uppermost in mind: What does the reader know so far? What does the reader expect next and why?

Treat the reader as you would a guest in your house

Anticipate their needs: would you like something to drink?
Something to eat? Perhaps now, after eating, you'd like to rest?



Writing style, from the elements of style, Stunk and White

13. Omit needless words.

Vigorous writing is concise. A sentence should contain no unnecessary words, a paragraph no unnecessary sentences, for the same reason that a drawing should have no unnecessary lines and a machine no unnecessary parts. This requires not that the writer make all his sentences short, or that he avoid all detail and treat his subjects only in outline, but that every word tell.

Many expressions in common use violate this principle:

the question as to whether	whether (the question whether)
there is no doubt but that	no doubt (doubtless)
used for fuel purposes	used for fuel
he is a man who	he
in a hasty manner	hastily
this is a subject which	this subject
His story is a strange one.	His story is strange.

Re-writing exercise

Text from a CVPR Workshop paper I'm co-author on.

The underlying assumption of this work is that the estimate of a given node will only depend on nodes within a patch: this is a locality assumption imposed at the patch-level. This assumption can be justified in case of skin images since a pixel in one corner of the image is likely to have small effect on a different pixel far away from itself. Therefore, we can crop the image into smaller windows, as shown in Figure 5, and compute the inverse J matrix of the cropped window. Since the cropped window is much smaller than the input image, the inversion of J matrix is computationally cheaper. Since we are inferring on blocks of image patches (i.e. ignoring pixels outside of the cropped window), the interpolated image will have blocky artifacts. Therefore, only part of xMAP is used to interpolate the image, as shown in Figure 5.

Re-writing exercise

Original:

The underlying assumption of this work is that the estimate of a given node will only depend on nodes within a patch: this is a locality assumption imposed at the patch-level. This assumption can be justified in case of skin images since a pixel in one corner of the image is likely to have small effect on a different pixel far away from itself.

Re-writing exercise

Original:

Therefore, we can crop the image into smaller windows, as shown in Figure 5, and compute the inverse J matrix of the cropped window. Since the cropped window is much smaller than the input image, the inversion of J matrix is computationally cheaper.

Re-writing exercise

Original:

Since we are inferring on blocks of image patches (i.e. ignoring pixels outside of the cropped window), the interpolated image will have blocky artifacts. Therefore, only part of xMAP is used to interpolate the image, as shown in Figure 5.

Re-writing exercise

The underlying assumption of this work is that the estimate of a given node will only depend on nodes within a patch: this is a locality assumption imposed at the patch-level. This assumption can be justified in case of skin images since a pixel in one corner of the image is likely to have small effect on a different pixel far away from itself. Therefore, we can crop the image into smaller windows, as shown in Figure 5, and compute the inverse J matrix of the cropped window. Since the cropped window is much smaller than the input image, the inversion of J matrix is computationally cheaper. Since we are inferring on blocks of image patches (i.e. ignoring pixels outside of the cropped window), the interpolated image will have blocky artifacts. Therefore, only part of xMAP is used to interpolate the image, as shown in Figure 5.

Before

We assume local influence--that nodes only depend on other nodes within a patch. This condition often holds for skin images, which have few long edges or structures. We crop the image into small windows, as shown in Fig. 5, and compute the inverse J matrix of each small window. This is much faster than computing the inverse J matrix for the input image. To avoid artifacts from the block processing, only the center region of xMAP is used in the final image, as shown in Fig. 5.

After

This editing benefits you twice: (1) you have 50% more space to tell your story, and (2) the text is easier for the reader to understand.

Figures and captions

It should be easy to read the paper in a big hurry and still learn the main points. **Probably most of your readers will be skimming the paper.**

The figures and captions can help tell the story.

So the figure captions should be self-contained and **the caption should tell the reader what to notice about the figure.**

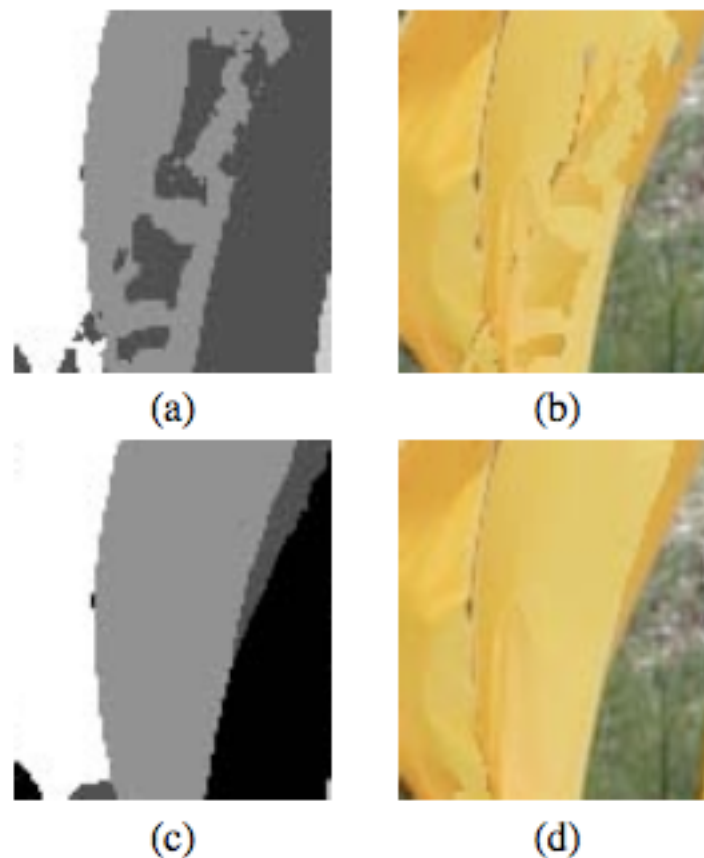


Figure 3: (a) Time-frame assignments for the front-most surface pixels, based on stereo depth measurements alone, without MRF processing. Grey level indicates the time-frame assignment at each pixel. (b) Shape-time image based on those assignments. (c) Most probable time-frame assignments, computed by MRF. (d) Resulting shape-time image. Note that the belief propagation in the MRF has removed spurious frame assignment changes.

Knuth on equations

13. Many readers will skim over formulas on their first reading of your exposition. Therefore, your sentences should flow smoothly when all but the simplest formulas are replaced by “blah” or some other grunting noise.

Mermin on equations

rule in your original manuscript.

Rule 2 (Good Samaritan rule). A Good Samaritan is compassionate and helpful to one in distress, and there is nothing more distressing than having to hunt your way back in a manuscript in search of Eq. (2.47) not because your subsequent progress requires you to inspect it in detail, but merely to find out what it is *about* so you may know the principles that go into the construction of Eq. (7.38). The Good Samaritan rule says: *When referring to an equation identify it by a phrase as well as a number.* No compassionate and helpful person would herald the arrival of Eq. (7.38) by saying “inserting (2.47) and (3.51) into (5.13) . . .” when it is possible to say “inserting the form (2.47) of the electric field \mathbf{E} and the Lindhard form (3.51) of the dielectric function ϵ into the constitutive equation (5.13)”



Tone: be kind and gracious

- My initial comments.
- My advisor's comments to me.

Image Quilting for Texture Synthesis and Transfer

Alexei A. Efros^{1,2}

William T. Freeman²

¹University of California, Berkeley

²Mitsubishi Electric Research Laboratories

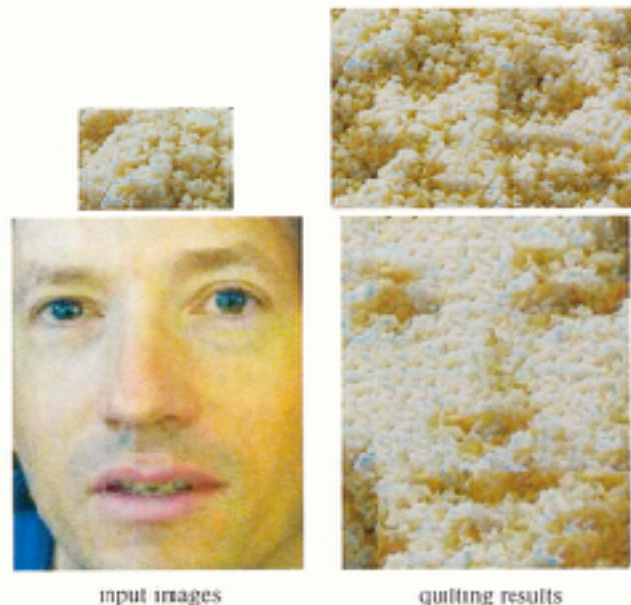
Abstract

We present a simple image-based method of generating novel visual appearance in which a new image is synthesized by stitching together small patches of existing images. We call this process *image quilting*. First, we use quilting as a fast and very simple texture synthesis algorithm which produces surprisingly good results for a wide range of textures. Second, we extend the algorithm to perform texture transfer – rendering an object with a texture taken from a different object. More generally, we demonstrate how an image can be re-rendered in the style of a different image. The method works directly on the images and does not require 3D information.

Keywords: Texture Synthesis, Texture Mapping, Image-based Rendering

1 Introduction

In the past decade computer graphics experienced a wave of activity in the area of image-based rendering as researchers explored the idea of capturing samples of the real world as images and using them to synthesize novel views rather than recreating the entire



Efros's comments within our texture synthesis paper about competing methods.

A number of papers to be published this year, all developed independently, are closely related to our work. The idea of texture transfer based on variations of [6] has been proposed by several authors [9, 1, 11] (in particular, see the elegant paper by Hertzmann et.al. [11] in these proceedings). Liang et.al. [13] propose a real-time patch-based texture synthesis method very similar to ours. The reader is urged to review these works for a more complete picture of the field.

Develop a reputation for being clear and reliable

(and for doing creative, good work...)

- There are perceived pressures to over-sell, hide drawbacks, and disparage others' work. Don't succumb. (That's in both your long and short-term interests).
- “because the author was [REDACTED], I knew I could trust the results.” [a conference chair discussing some of the reasons behind a best paper prize selection].

Be honest, scrupulously honest

Convey the right impression of performance.

MAP estimation of deblurring. We didn't know why it didn't work, but we reported that it didn't work. Now we think we know why. Others have gone through contortions to show why they worked.

Author order

- Some communities use alphabetical order (physics, math).
- For biology, it's like bidding in bridge.
- Engineering seems to be: in descending order of contribution.
- Should the advisor be on the paper?
 - Did they frame the problem?
 - Do they know anything about the paper?
 - Do they need their name to appear on the papers for continued grant support?

My experiences with having names on papers

Author list

- My rule of thumb: All that matters is how good the paper is. If more authors make the paper better, add more authors. If someone feels they should be an author, and you trust them and you're on the fence, add them
- It's much better to be one of many authors on a great paper than to be one of just a few authors on a mediocre paper.
- The benefit of a paper to you is a very non-linear function of its quality:
 - A mediocre paper is worth nothing.
 - Only really good papers are worth anything.

Title?



IEEE TRANSACTIONS ON

INFORMATION THEORY

MARCH 1992 VOLUME 38 NUMBER 2 (PART I) [ISSN 0018-9448]

A JOURNAL DEVOTED TO THE THEORETICAL AND EXPERIMENTAL ASPECTS OF INFORMATION THEORY, CODING, PROCESSING, AND COMMUNICATION
PART I OF TWO PARTS

SPECIAL ISSUE ON WAVELET TRANSFORMS AND MULTIREOLUTION SIGNAL ANALYSIS

F. Heurich, S. Mallat, and A. J. E. Bellamy	Introduction to the Special Issue	719
PAPERS		
Theory and Implementation of Wavelet and Multiresolution Transforms		
A. Antoniou and M. Pitscheks	Nonadaptive Multiresolution Perfect Reconstruction Biorthogonal Wavelets for Discrete Multiresolution Analysis, Haar Bases, and Self-Similar Tilings of \mathbb{R}^n	213
K. Ochi and H. N. Nagar	Fast Algorithms for Discrete and Continuous Wavelet Transforms	219
G. Muelhalp and P. H. Geisel	Self-Similar Multiresolution Transforms	257
E. J. Schemmel, W. F. Swenson, C. S. Adcock, and R. J. Whelan	Noise Resilience in Tight Wavelet-Haarwavelet Frames	638
W. J. Alcock	Time-Frequency and Invariant Analysis	651
S. Mallat and R. J. Whelan	Stable and Unstable Invariant Wavelets	677
W. Seregin, A. Kravtsov, E. G. Viorato, P. Kozmar-Moravcsik, R. Toloczko, and M. Turbell	Asymptotic Moment and Order Analysis: The Solution of Integro-differential Equations	684
A. P. Yezhov and A. P. Yezhov	Performance Analysis of Turbulent Channels Based on a Class of Linear Wavelet Transforms	697
R. Klette, J. A. Cahoy, and P. W. S. Lee	A Generalized Wavelet Transform for Fourier Analysis: The Multiresolution Invariant Transform and Its Application to Image and Audio Signal Analysis	671
A. C. Bovik, M. Gopal, T. Sengocak, and J. R. Mersero-Petersen	Localized Measurement of Emergent Image Fractalness by Gabor Wavelets	681
Compressive and Efficient Representations		
M. R. Cozzolino and M. P. P. Vetro	Energy-Based Algorithms for Two-Basis Representations	717
R. J. DeVore, M. A. Bennett, and R. J. DeVore	Image Compression Through Wavelet Transform Coding	712
A. M. Tesch, M. Stuber, and P. Poggiolini	On the Optimal Choice of a Wavelet for Sparse Representation of Multiresolution Stochastic and Partially Noisy	747
M. Sorensen, A. Zemanek, K. C. Cill, C. J. Goble, R. Woodhead, and A. K. Pitts	Modeling and Estimation of Multiresolution Stochastic Processes	769
C. B. Kocch and J. P. O'Sullivan	Wavelet-Based Representations for a Class of Self-Similar Signals with Application to Packet Multicast	783
P. M. B. J. J. Van Veen and G. J. S. Ouyang	A Method of Moments for Multiresolution Spectrum Estimation and Filter Design	809
A. J. C. Cook	A Local-Global, Band-Separating, Bandwidth-Adaptability Transform Applied to Stochastic Gaussian Processes	814
Applications to Wavelet Transforms		
J. Yang, L. Wang, and S. J. Shensa	Adaptive Representation of Time-Varying Signals	824
D. M. Leahy and J. B. Pender	The Application of Wavelet Transforms to Hyperspectral Image Processing	843

Our title

- Was:
 - Shiftable Multiscale Transforms.
- Should have been:
 - What's Wrong with Wavelets?

How papers are evaluated

After the papers come in:

- Program chairs assign each paper to an area chair.
- Area chairs assign each of their papers to 3 (or for SIGGRAPH, 5) reviewers.
- Reviewers read and review 5 – 15 papers.
- Authors respond to reviews.
- Area chairs read reviews and author/reviewer dialog and look at paper and decide whether to reject or accept as poster or oral talk. The area chair may have 30 or so papers to handle.

Strategy tips

From an area chair's point of view, the types of papers in your pile

- About 1/3 are obvious rejects
- In the whole set, maybe 1 is a really nice paper--well-written, great results, good idea. That will be an oral presentation.
- The rest are borderline, and these fall into two camps...

From an area chair's point of view, the
two types of borderline papers...

Quick and easy reasons to reject a paper

With the task of rejecting at least 75% of the submissions, area chairs are groping for reasons to reject a paper. Here's a summary of reasons that are commonly used:

- Do the authors not deliver what they promise?
- Are important references missing (and therefore one suspects the authors not up on the state-of-the-art for this problem)?
- Are the results too incremental (too similar to previous work)?
- Are the results believable (too different than previous work)?
- Is the paper poorly written?
- Are there mistakes or incorrect statements?

Sources on writing technical papers

- How to Get Your SIGGRAPH Paper Rejected, Jim Kajiya, SIGGRAPH 1993 Papers Chair, <http://www.siggraph.org/publications/instructions/rejected.html>
- Ted Adelson's Informal guidelines for writing a paper, 1991. <http://www.ai.mit.edu/courses/6.899/papers/ted.htm>
- Notes on technical writing, Don Knuth, 1989.
<http://www.ai.mit.edu/courses/6.899/papers/knuthAll.pdf>
- What's wrong with these equations, David Mermin, Physics Today, Oct., 1989. <http://www.ai.mit.edu/courses/6.899/papers/mermin.pdf>
- Notes on writing by Fredo Durand, people.csail.mit.edu/fredo/PUBLI/writing.pdf and Aaron Hertzmann, <http://www.dgp.toronto.edu/~hertzman/advice/writing-technical-papers.pdf>
- Three sins of authors in computer science and math, Jonathan Shewchuck, <http://www.cs.cmu.edu/~jrs/sins.html>
- Ten Simple Rules for Mathematical Writing, Dimitri P. Bertsekas http://www.mit.edu:8001/people/dimitrib/Ten_Rules.html

Outline

- writing technical papers
- giving technical talks



How to give talks

- Giving good talks is important for a researcher.
- You might think, “the work itself is what really counts. Giving the talk is secondary”.
- But the ability to give a good talk is like having a big serve in tennis—by itself, it doesn’t win the game for you. But it sure helps. And the very best tennis players all have great serves.
- Researchers as little corporations.



Sources on giving talks

Patrick Winston's annual IAP talk on how to give talks.

Books on speaking.

Suggestions from your advisor or helpful audience members.

Analyzing good talks that others give.

High order bit: prepare

- Practice by yourself.
- Give practice versions to your friends.
- Think through your talk.
- You can write out verbatim what you want to say in the difficult parts.
- Ahead of time, visit where you'll be giving the talk and identify any issues that may come up.
- Preparation is a great cure for nervousness.



A tip to not be nervous that I found useful

- Get over it. They're not there to see you, they're there to hear the information. Just convey the information to them.

The different kinds of talks you'll have to give as a researcher

- 2-5 minute talks
- 10 -20 minute conference presentations
- 30-60 minute colloquia

Very short talks

- Rehearse it.
- Cut things out that aren't essential. You can refer to them at a high level.
- You might focus on answering just a few questions, eg: what is the problem? Why is it interesting? Why is it hard?
- Typically these talks are just little advertisements for a poster or for some other (longer) talk. So you just need to show people that the problem is interesting and that you're fun to talk with.
- These talks can convey important info--note popularity of SIGGRAPH fast forward session.

Recommendation

- For your five-minute talks, write down:
 - what problem did you address?
 - why is it interesting?
 - why is it hard?
 - what was the key to your approach?
 - how well did it work?

The different kinds of talks you'll have to give as a researcher

- 2-5 minute talks
- 10-20 minute conference presentations
- 30-60 minute colloquia



David Jacob's bad news

The more you work on a talk, the better it gets: if you work on it for 3 hours, the talk you give will be better than if you had only worked on it for 2 hours. If you work on it for 5 hours, it will be better still. 7 hours, better yet...



(told to me by David on a beach in Greece, a few hours before my oral presentation at ICCV. That motivated me to leave the beach and go back to my room to work more on my talk, which paid off).

Figure out how one part follows from another

Ahead of time, think through how each part motivates the next, and point that out during the talk. If one part doesn't motivate the next, consider re-ordering the talk until it has that feel.

Your audience

- Your image of your audience:
 - Paying attention, listening to every word
- Your audience in reality:
 - Tired, hungry, not wanting to sit through yet another talk at the conference...

Layering the talk. When we read a paper, headings and sections help us follow the paper. You should provide the verbal equivalents of headings to the listener.



http://tbn0.google.com/images?q=tbn:4oWYOjaSp4vopM:http://bakery.grillsforallseasons.com/photos/wedding_cake3.jpg

The probability of an observation has three terms to it.

Blah blah blah blah blah blah blah blah blah blah
blah blah blah blah blah blah blah blah blah blah
blah blah blah blah blah blah blah blah blah blah
blah blah blah

So that gives us the objective function we want to optimize. Now, how do we find the optimal value?

There are two approaches you can take. blah blah blah
blah blah blah blah blah blah blah blah blah blah
blah blah blah blah blah blah blah blah blah blah
blah blah blah blah blah

So now, with these tools in hand, we can apply this methods to real images. blah blah blah blah blah
blah blah blah blah blah blah blah blah blah blah

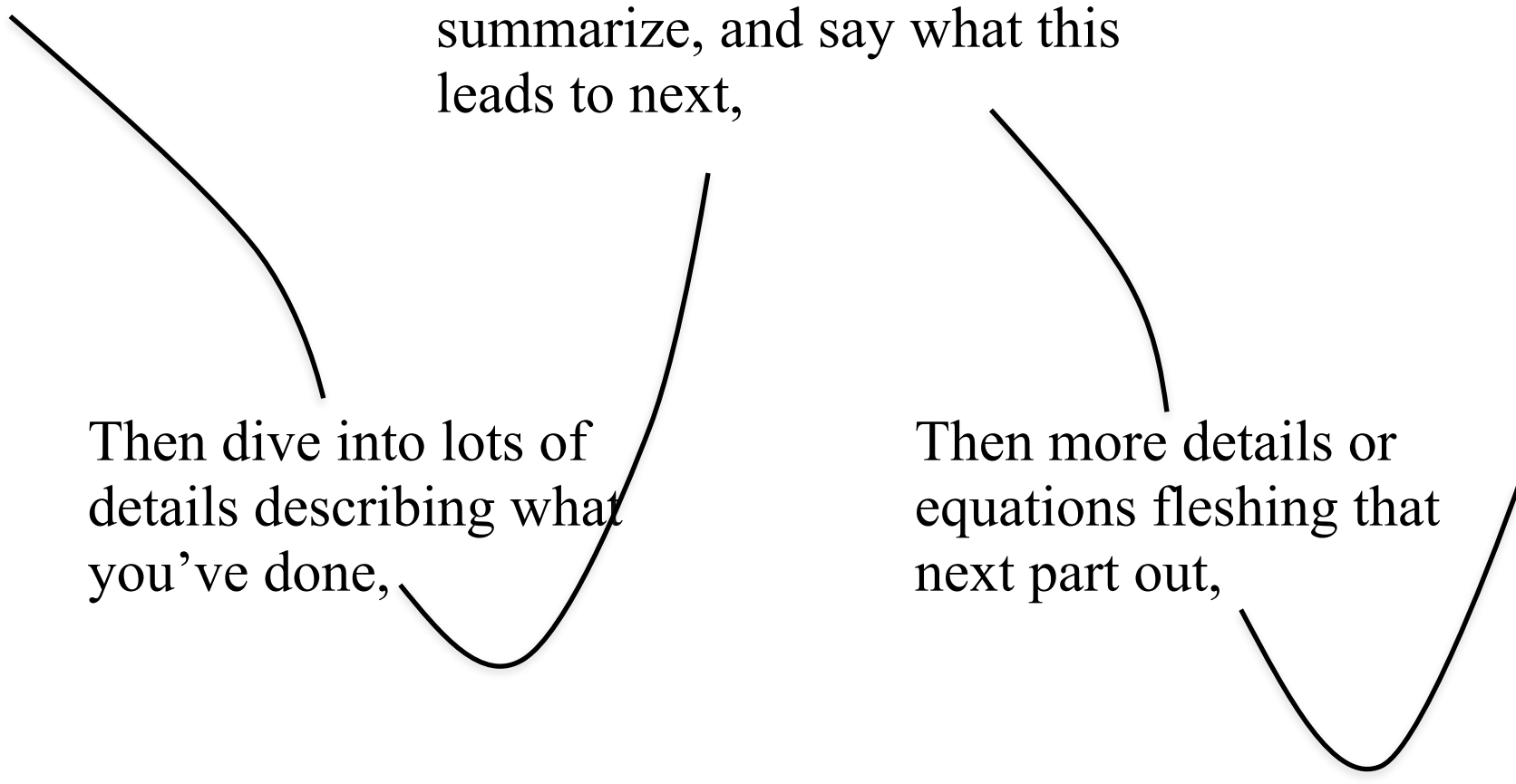
You tell the story at several different levels of detail

The main idea

Then come up for air,
summarize, and say what this
leads to next,

Then dive into lots of
details describing what
you've done,

Then more details or
equations fleshing that
next part out,



Ways to engage the audience

- So you've been talking on and on. You want to break things up and keep the audience engaged. Can you think of a way to bring the audience into the talk?
- Demos can also help.
- Or add audience participation components to the talk. For human or computer vision talks, you can often present to the audience what the task is that the human or computer has to solve.
- The audience loves to figure things out, to solve puzzles, to make guesses. Feed those desires.
- The response-meter.

Ted Adelson

- “people like to see a good fight”
- The flat earth theory predicts that ships will appear on the horizon as small versions of the complete ship. Under that theory, you’d expect approaching ships to look like this:



Present a fight

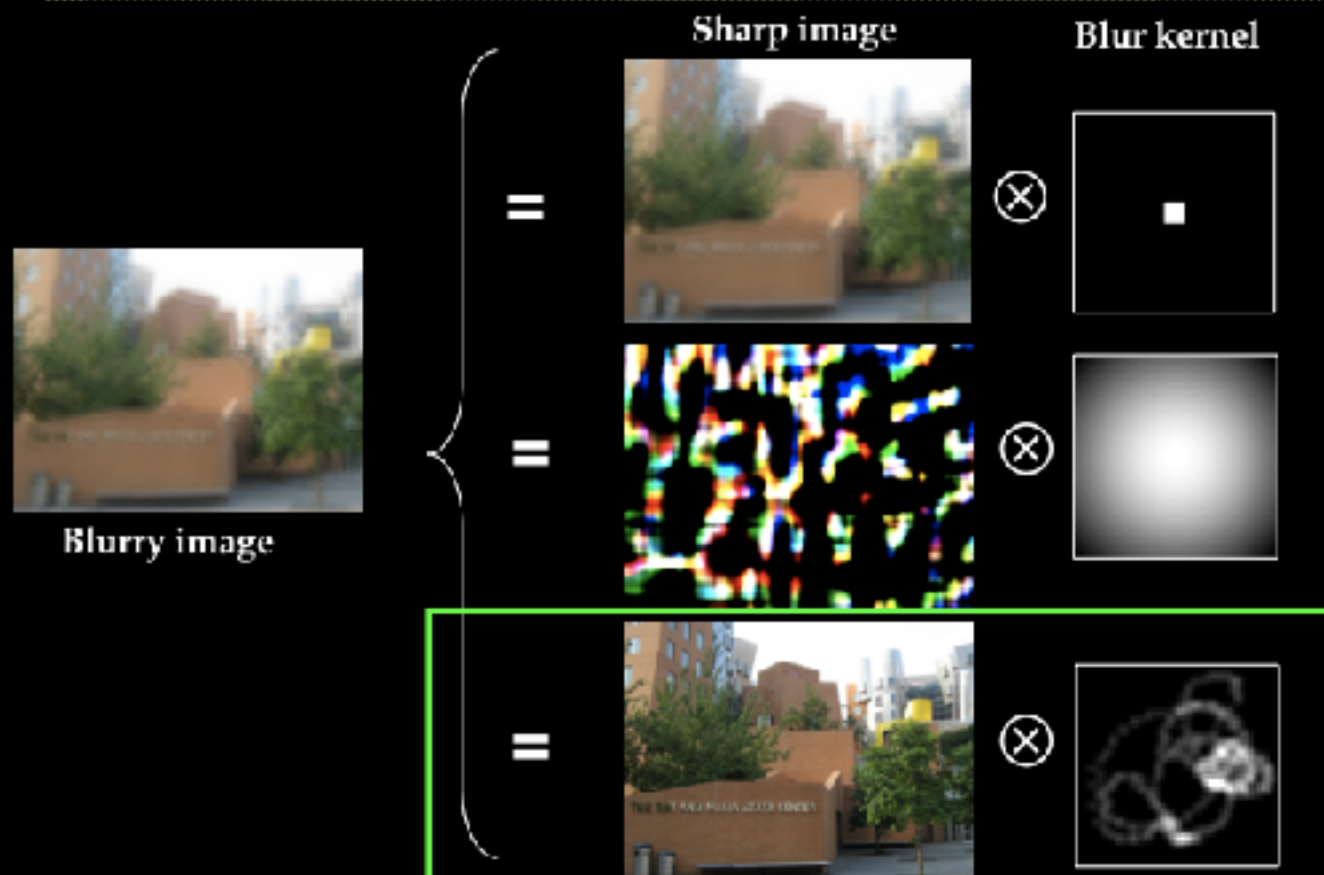
Whereas the round earth theory predicts that the top of the sails will appear first, then gradually the rest of the ship below it.





[http://www.flickr.com/photos/mnsomero/
2738807250/](http://www.flickr.com/photos/mnsomero/2738807250/)

Multiple possible solutions



What I think the audience wants

To have everything follow and make sense

To learn something

To connect with the speaker, to share their excitement.

They want to watch you love something!

Alan Alda's comments (see <http://mcgovern.mit.edu/video-gallery>, starting at 18 minutes in (but earlier is good, too).)

Present to the mean.

Let the audience see your personality

- They want to see you enjoy yourself.
- They want to see what you love about the work.
- People really respond to the human parts of a talk. Those parts help the audience with their difficult task of listening to an hour-long talk on a technical subject. What was easy, what was fun, what was hard about the work?
- Don't be afraid to be yourself and to be quirky.



How to end a talk

- People often say “are there any questions?” but then people don’t know whether to applaud or to raise their hand.
- If you say “thank you”, then everyone knows that they’re supposed to applaud now. After that is over, then you can ask for questions.